Heavy-ion storage-ring-lifetime measurement of metastable levels in the C-, N-, and O-like ions of Si, P, and S

E. Träbert
Astronomisches Institut, Ruhr-Universität Bochum, D-44780 Bochum, Germany

M. Grieser, J. Hoffmann, C. Krantz, R. Repnow, and A. Wolf
Max-Planck-Institut für Kernphysik, D-69117 Heidelberg, Germany

(Received 8 March 2012; published 6 April 2012)

In a quest for benchmarking transition rate data on electric-dipole ($E1$) forbidden transitions to be used in collisional-radiative models of plasma spectra, the radiative decay rates of the metastable levels $2s^2 2p^2\ ^1D_2$, $2s^2 2p^3\ ^2P^o_{1/2,3/2}$, and $2s^2 2p^4\ ^1D_2$ in C-, N-, and O-like ions, respectively, have been measured for the elements Si, P, and S. Results with uncertainties mostly well below 1% are obtained using ions circulating in a storage ring. Precision results for Si^{7+}, P^{7+}, P^{8+}, P^{9+}, S^{8+}, and S^{10+} obtained here complete the isoelectronic sequence data sets for these four metastable levels in all three elements.

DOI: 10.1103/PhysRevA.85.042508 PACS number(s): 32.70.Cs, 32.30.Jc, 34.50.Fa

I. INTRODUCTION

The ground configurations of many-electron atomic systems, beginning with the doublet ground term of B-like (five-electron) ions, harbor a number of levels. The transition rates between these levels are low, because the transition energies are low and because the usually dominant electric dipole ($E1$) transitions are ruled out by the same parity of initial and final states. Hence magnetic dipole ($M1$) and electric quadrupole ($E2$) transitions dominate. Representing the very first excited levels of a given ion, such transitions have long been used as indicators that a given ionization stage of a given elemental species is present in a plasma [1,2], and thus the plasma (electron) temperature must be sufficiently high and can be estimated. However, the optical spectra carry more information [3,4]. In particular in a dilute plasma, the collision frequency competes with the radiative decay rate, and then the relative population of levels within the ground configuration (notably fine-structure levels of the ground term, for example, in C- and O-like ions) may depend on the electron density. On the other hand, if the first-level interval is relatively large (as, for example, in N-like ions), the level populations of the upper levels of the ground configuration compared to that of the true ground level depend significantly on the plasma temperature.

One approach in plasma diagnostics measures the line ratios of lines that depend on the level populations of low-lying levels. For this procedure, collisional-radiative models have been developed that include thousands of levels and tens of thousands of transitions between mostly high-lying levels; such models are used to provide synthetic spectra and to learn about their dependence on density and temperature. Most of the atomic data used in such models are obtained by calculation only, since experiment cannot practically provide the vast amount of information. However, the excitation energies of low-lying and resonance levels are usually better obtained from spectroscopic experiment, and the calculated energy scale is regularly corrected for experimental data. Also, a number of $E1$ transition rates are available from beam-foil spectroscopy, in most cases at moderate precision (level lifetimes in the range from a few picoseconds to many nanoseconds, typically measured with a precision of 5% to 10%). The measurement of the much-longer-lived levels in the ground configurations (lifetimes in the millisecond to second range, for low to moderate charge states) requires ion trapping techniques.

In about the last decade, experiments at heavy-ion storage rings and at electron beam ion traps have provided such lifetime data [5–8] with accuracies of usually between 3% and 0.3% (and in some cases even better than that, see examples in Ref. [9]). In the early measurements, priority was given to specific cases of particular interest (plasma diagnostics, astrophysics); by now the data extend over sections of isoelectronic ranges and begin to permit one to look into further questions: With the growing experience and confidence in highly accurate measurements, does the systematic error scenario need to be reassessed? Do measurements on several ion species reveal new problems that may have been overlooked initially; does theory hold up with the best experiments? Do data on isoelectronic sequences perhaps reveal shortcomings in individual measurements or calculations? What obstacles can be identified on the way to testing the accuracy limits of calculations of transition rates, recognizing that two of the most accurate lifetime measurements [10–12] disagree with the results of extensive calculations at a level larger than the QED correction to the magnetic-dipole ($M1$) transition probability [10,13]?

Not all of these questions can be answered in a single experiment. Ions with an open L shell may be more conducive to high accuracy studies, since recent work on M shell ions—though using the very same experimental techniques—has found complications due to the level structure that appear to limit the accuracy of lifetime measurements there [9,14]. About a decade ago we have measured the radiative lifetimes of the $2s^2 2p^2\ ^1D_2$ level in the C-like ion Si^{8+}, of the $2s^2 2p^3\ ^2P^o_{1/2,3/2}$ level in the N-like ion S^{9+}, and of the $2s^2 2p^4\ ^1D_2$ level in the O-like ion Si^{6+} [15,16], with an uncertainty of about 1%. The level structure and the transitions of interest are sketched in Fig. 1. We now have extended these heavy-ion storage-ring measurements to the same levels in the isoelectronic ions of Si, P, and S, with even better statistical reliability of the data and with the consistency check provided by isoelectronic data

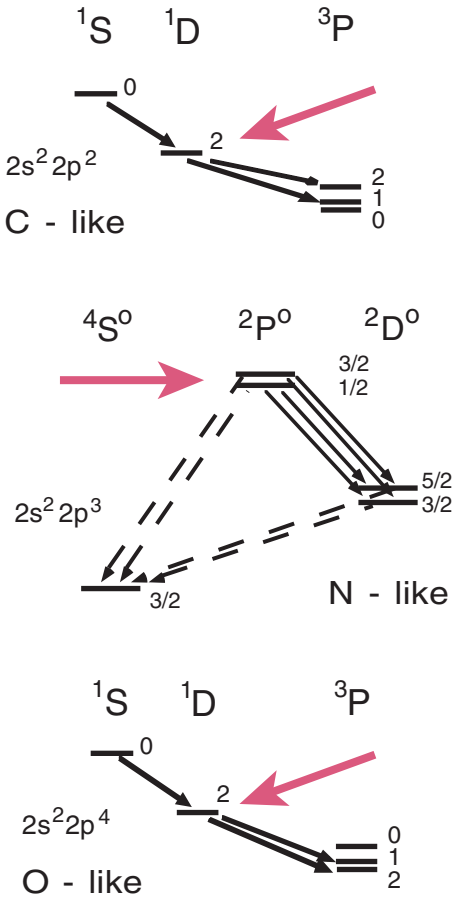

FIG. 1. (Color online) Level schemes and major transitions in the ground configurations of C-, N-, and O-like ions. The level positions depicted are not to scale with the actual level energies. The large pink arrows point to the levels presently measured.

sets. We discuss our experimental observations and compare our results to various predictions.

II. EXPERIMENT

Our experiment employed the heavy-ion storage ring TSR [17,18] at Heidelberg, using the procedures described in more detail previously [15,19,20]. Beams of the desired ions (for beam energies and other parameters, see Table I) were provided by a tandem accelerator (with a foil stripper in the high-voltage terminal) and injected into the storage ring. The ion energies were chosen for optimum ion production and for time-saving changeovers between the ion beams, employing the same magnet settings of the heavy-ion storage ring for several ion species when feasible. By the multiturn injection technique (accumulation of ions in the ring aided by slightly displacing the trajectory of already stored ions [21]), electrical ion beam currents of up to 40 μA for Si^{7+}, up to 70 μA for P^{7+}, and up to 190 μA for S^{8+} were reached (corresponding to particle currents of some 6 to 24 μA), and values were of the same order of magnitude for the other ion species. Then the ion injection was stopped and the ions were left coasting for 200 ms before the ions were ejected and the storage ring was refilled. During the coasting period, photons emitted by the stored ions were detected by a solar blind photomultiplier (EMR 541 Q) with a dark rate of 1 count/s. This device detected light between the cutoff wavelength of the sapphire window of the storage-ring vacuum vessel (sapphire has a soft absorption edge near the short-wavelength cutoff at about 165 nm) up to about 280 nm. For P^{7+}, the wavelengths of interest, the decay branches of the $2s^2 2p^4\ {}^1D_2$ level to the $^3P_1$ and $^3P_2$ levels are 191.4 and 215 nm; for S^{8+} the two lines are at 171.5 and 198.8 nm, respectively. The 171.5 nm light encounters some absorption in the vacuum vessel window and in the about 1 cm of air between the window and the entrance window to the photomultiplier tube, which resulted in a lower signal-to-noise rate. In Si^{7+}, the decay branches of the $2s^2 2p^3\ {}^2P^o_{1/2,3/2}$ level that fall into the detection range of the solar blind photomultiplier are near 272, 274, and 276 nm, all of which are on the steep slope of diminishing sensitivity of this detector's photocathode material. Consequently the signal rate was lowest in this last example, even though the ion beam current was high. The light from the transitions of interest in the other ion species was less affected by the limits of the detector working range; all wavelengths are listed in Table I.

The signal was sorted into 200 channels of 1 ms width each; the total accumulation time per channel was 470 s for P^{7+} and 220 s for S^{8+}, respectively (for further such values, see Table I). The sum of all our decay data on S^{8+} is shown in Fig. 2, which is typical of our data. Every minute the new data were written to a storage medium, so that afterward data records for times when, for example, the stored ion beam was much below average could be removed from the record. The

TABLE I. List of transitions studied for C-, N-, and O-like ions in previous work (references given) and in the present measurement (parameters listed).

Ion	Level	Wavelength (nm)	Ion beam energy (MeV)	Particle current (μA)	Ion beam lifetime (s)	Accumulation time per channel (s)	Ref.
Si^{8+}	$2s^2 2p^2\ {}^1D_2$	198/215					[15]
P^{9+}		179/198	100.6	7.5	69	390	
S^{10+}		161/183	42.3	18	65	398	
Si^{7+}	$2s^2 2p^3\ {}^2P^o_{1/2,3/2}$	272–276	56	3–5	45	195	
P^{8+}		242–249	79.5	3.5–8	34	365	
S^{9+}		223–226					[16]
Si^{6+}	$2s^2 2p^4\ {}^1D_2$	208/228					[15]
P^{7+}		191/215	74.8	10	5.7	470	
S^{8+}		171/199	95	24	14.6	220	

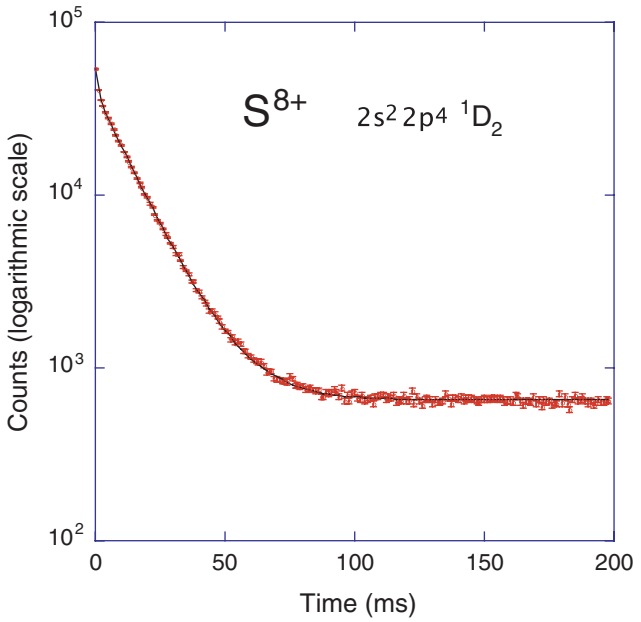

FIG. 2. (Color online) Decay curve of the $2s^2 2p^4\ ^1D_2$ level in S^{8+} and two-exponential fit to the data. The data accumulation time per 1 ms wide channel is 220 s.

total signal above background amounted to about 1.2 million counts for P^{7+} (0.5 million counts for S^{8+}, and a similar order of magnitude for most of the other ions) and a peak signal to dark rate ratio ranging from 60 to 200 for the different ions. On purely statistical grounds, all data sets were sufficient to determine the time constant of a single exponential decay to better than 0.3% uncertainty.

The apparent decay rate of the signal is the sum of the radiative decay rate and the ion loss rate, that is, the reduction of the number of stored ions by various collision types. The ion loss rate was determined apart from the actual radiative decay measurements, by measuring (with a current transformer) the stored ion beam current over periods of about 1 min. The rate coefficient for ion loss is a steep function of ion velocity; in our experiment, the ion beam lifetime ranged from 5.7 s (P^{7+}) and 14.6 s (S^{8+}) to 45 s (Si^{7+}), strongly dependent on the ion beam energy. There also is a beam profile monitor, based on the ionization of residual gas particles by the stored ion beam, that measures the ion beam current and its variation on somewhat shorter time scales. Nevertheless, even this device is not designed to cope with fast transients. Hence the accuracy of ion loss measurements during the 200-ms photon measurement interval is limited. We therefore apply the correction suggested by the transformer measurement, but adopt half of the correction as the uncertainty measure of the procedure. The phosphorus (P^{7+}) measurement, for example, needs a correction for sample loss by 0.5%; the associated uncertainty of 0.25% is significantly larger than the statistical uncertainty (0.1%) of the photon signal. For some of the ion species with longer storage time constants, the correction amounted to less than 0.1% and was then smaller than the statistical uncertainty or the correction for relativity: relativistic time dilation requires a correction of opposite sign; for example, the γ factor was 1.0026 for P^{7+} and 1.0032 for S^{8+}. The corrections for all ion species studied are listed in Table II.

III. DATA

The data curves were fitted by one or two exponentials plus a constant background. Fits with a single exponential worked well (reduced χ^2 value $\approx$1) where a single exponential decay was expected (for C- and O-like ions), but failed—as expected—to match the decay curve shape for N-like ions (with two fine-structure levels). Fit attempts testing for the possible presence of cascade contributions or spectral blends by introducing an additional decay component gave no indication of a statistically merited further decay contribution except in the one case discussed below. As a second test for additional decay components with a decay time constant possibly close to the one (or two) of interest, and to check for possible distortions of the decay curves at ion injection, decay curves were analyzed by successively truncating early data channels up to 10, 20, or 30 ms, depending on the magnitude of the radiative lifetime in question. The first channel of all data relates to the time when the old ion cloud is dumped from the storage ring, and the fresh 70-turn injection then takes less than a millisecond. The eventually stored ion beam current is lower than the factor of 70 over the single-turn injection beam

TABLE II. Lifetime results for C-, N-, and O-like ions from previous work (references given) and from the present work, including correction factors as explained in the text. For N-like ions, the decay curves consist of a superposition of the decays of two upper levels, and thus two components have to be extracted from the decay curves.

Ion	Level	Beam lifetime correction factor[a]	Gamma factor	Radiative lifetime (ms)	Ref.
Si^{8+}	$2s^2 2p^2\ ^1D_2$			38.3 ± 0.3	[15]
P^{9+}		1.0003	1.00348	17.74 ± 0.035	This work
S^{10+}		1.0001	1.00142	8.684 ± 0.009	This work
Si^{7+}	$2s^2 2p^3\ ^2P^o_{1/2,3/2}$	1.00025	1.00215	$23.5 \pm 1 / 9.63 \pm 0.3$	This work
P^{8+}		1.00012/1.00033	1.00274	$10.20 \pm 0.12 / 4.24 \pm 0.10$	This work
S^{9+}				$5.20 \pm 0.15 / 2.10 \pm 0.06$	[16]
Si^{6+}	$2s^2 2p^4\ ^1D_2$			63.6 ± 0.7	[15]
P^{7+}		1.005	1.00259	28.57 ± 0.08	This work
S^{8+}		1.001	1.00319	13.61 ± 0.05	This work

[a]Correction for ion loss from the stored sample (see Sec. II).

TABLE III. Experimental lifetime results (ms) for the $2s^2 2p^2\ ^1D_2$ level in the C-like ions Si^{8+} [15], P^{9+}, and S^{10+} (this work) and theoretical predictions from the references listed.

Si^{8+}	P^{9+}	S^{10+}	Ref.
	Experiment		
38.3 ± 0.3	17.74 ± 0.035	8.684 ± 0.009	
	Theory		
37.17			[31]
32.95	15.49	7.69	[24]
38.97	17.99	8.77	[32]
38.04			[33]
37.45	17.30	8.44	[34]
41.25	19.04	9.32	[34][a]
38.91	18.05	8.84	[26]
39.99	18.44	9.00	[35]
39.60	18.23	8.87	[29]
38.18–38.44	17.64–17.75	8.601	[36]
38.70	17.88	8.734	[37]
38.99	18.48	8.77	[30]
38.53	17.83	8.71	[38]

[a]Corrected by [29].

current, so some ion losses incur in the multiturn injection process in which the ion trajectories are slightly displaced after each turn so that another segment of the phase space can be filled. The data evaluation of stepwise truncation showed stable results after truncating three channels (3 ms in the data set or 2 ms after the beginning of injection). The lifetime results quoted are those of a sliding average over these evaluations, with a statistical error indicated by the fits beginning at early channels. These results were then corrected for relativistic time dilation (on the order of 2 to 3 parts in a thousand) and for the ion loss rate from the stored sample, the inverse of the ion storage time constant (a correction on the order of 10^{-3} to some 10^{-4} in most cases studied here). The fit results and corrections as well as the final results and their uncertainties are listed in Table II.

All three elements studied presently are suitable to obtain high ion beam currents in a heavy-ion tandem accelerator and actually reached multi-microampere particle currents in the heavy-ion storage ring, a prerequisite for a sufficiently high signal-to-noise ratio in passive photon observations of such stored ion beams. All decays in the present study entail uv and vuv wavelengths that could be observed with the same solar blind, low-noise photomultiplier tube, and the radiative lifetimes are near the optimum for any such studies, because the ion loss rate from the stored sample was so small that the associated correction (and its uncertainty) remained smaller than the already small statistical uncertainty and the relativistic correction. The counting statistics was, in fact, so good that, in the case of the N-like ions with the two fine-structure levels that differ in lifetime merely by a factor of about 2.5, the fit algorithm found stable results (as a function of the starting channel) without difficulty. However, the associated uncertainties of the results are much larger (several percent) than in the C- and O-like ions (a fraction of 1%, with about the same signal rate and data statistics) due to the fact that the lifetime values of the two simultaneously fitted decay components are so close to each other (4.24 and 10.2 ms in P^{8+}, 9.63 and 23.5 ms in Si^{7+}).

In the decay curves of the C-like ions P^{9+} and S^{10+}, the single decay component of about 18- and 9-ms lifetime, respectively, belongs to the $2s^2 2p^2\ ^1D_2$ level of primary interest. In the decay curves of the O-like ions P^{7+} and S^{8+}, the dominant decay component of about 28- and 13-ms lifetime, respectively, is easily identified with the $2s^2 2p^4\ ^1D_2$ level of primary interest.

A. Fast decay component in O-like ions

Only in the decay curves of the latter two O-like ions there is also a much weaker fast component with a lifetime of order 1 ms. In several of our earlier measurements, such a component has been associated with the settling down of the circulating ion cloud right after injection into the storage ring. Such a transient ends within 1 or 2 ms. In the present cases, however, when truncating the first few channels of a decay curve and fitting the remainder of the data curves, single-exponential fits continued to show a slight trend toward longer lifetimes with the successive truncation of early data channels, which is inconsistent with the scenario of distortions at ion injection. Such a drawn-out lifetime effect may result from either a

TABLE IV. Experimental lifetime results (ms) for the $2s^2 2p^3\ ^2P^o_{1/2,3/2}$ levels in the N-like ions Si^{7+}, P^{8+} (this work), and S^{9+} [16], as well as theoretically predicted values.

Si^{7+}	P^{8+}	S^{9+}	Ref.
	Experiment		
$23.5 \pm 1.0/9.63 \pm 0.7$	$10.17 \pm 0.12/4.22 \pm 0.10$	$5.20 \pm 0.15/2.10 \pm 0.06$	
	Theory		
21.7/8.80	9.95/4.05	4.86/2.00	[24]
22.8/9.29	10.5/4.28	5.12/2.11	[4]
22.5/9.29	10.4/4.30	5.06/2.11	[39]
24.1/9.78			[40]
19.4/7.90	9.04/3.70	4.50/1.84	[26]
23.0/9.72	10.5/4.35	5.10/2.13	[41]
23.6/9.67	10.9/4.44	5.28/2.16	[42]
22.8/9.32–9.34	10.45/4.29	5.085/2.10	[43]
23.2/11.54	13.2/5.64	5.08/2.10	[30]

spectral blend with a somewhat faster (or slower) other decay or from cascade repopulation. In iron group ions with an open $3d$ shell, metastable levels have been identified that cause such a slow level repopulation [14], but no such levels have yet been found to affect ions with an open $n = 2$ shell. Fits beginning with with two exponentials of rather similar time constant or with a much slower second decay component did not reveal any stable solution for a second decay component.

In beam-foil spectroscopy, pico- and nanosecond decay curves have often been plagued by the so-called yrast tail, a decay chain along the levels of maximum angular momentum ℓ for a given principal quantum number n, as well as by the presence of some relatively long-lived cascade levels [22]. Estimates of the motional electric fields (on the order of 10^7 V/m) experienced by the fast ions in the magnetic dipole fields of the storage ring (magnetic field on average near 0.7 T) indicate that levels above $n = 50$ would largely be field ionized. According to a semiempirical formula by Omidvar [23], the unperturbed lifetimes of $n = 50$ yrast levels would be close to 6 μs in P^{7+} and close to 4 μs in S^{8+}. This falls 3 orders of magnitude short of the time range needed to explain the lifetime trend observed.

This leaves the possibility of a blend with a shorter-lived level decay. The only other long-lived (millisecond lifetime) level beyond the ground term that is known in O-like ions is the $2s^2 2p^4\ {}^1S_0$ level which predominantly decays at short wavelengths that should largely be blocked by the sapphire windows of the vacuum vessel and the photomultiplier tube. However, a weak decay branch of the ${}^1S_0$ level to the ${}^1D_2$ level of primary interest has been predicted at a branch fraction of about 1.5% in P^{7+} and about 1% in S^{8+} [24–30], with upper level lifetimes of about 2.8 to 3.1 ms and 1.35 to 1.5 ms in the two ions, respectively. The wavelengths of these decay branches (170.8 and 155.6 nm, respectively) are just inside and at the edge of the transmission range of the sapphire window of the storage-ring vacuum vessel. The decays are too fast and too weak in comparison with the dominant signal (and coincide with the aforementioned injection transient) to be evaluated for a meaningful lifetime measurement of the ${}^1S_0$ level, but their presence is evident. In the final data evaluation, a fast component was maintained at a fixed lifetime near the theoretical ${}^1S_0$ level lifetime prediction. Then the principal fit component was basically stable within the expected statistical scatter. The fit results, however, carry a somewhat increased uncertainty because of the need to take into account a second decay component.

As mentioned before, the fit results (apparent lifetimes) have to be corrected for the ion beam storage time constant (a 0.2% correction in P^{7+} and 0.1% in S^{8+}) and for relativistic time dilation. The results are compared with predictions in Tables III, IV, and V.

TABLE V. Experimental lifetime results (ms) for the $2s^2 2p^4\ {}^1D_2$ level in the O-like ions Si^{6+} [15], P^{7+}, and S^{8+} (this work), as well as theoretical predictions.

Si^{6+}	P^{7+}	S^{8+}	Ref.
	Experiment		
63.6 ± 0.7	28.63 ± 0.08	13.79 ± 0.05	
	Theory		
54.1	24.5	11.9	[24]
67.4	27.9	13.4	[25]
67.9	30.3	14.4	[25][a]
61.8	27.8	13.3	[26]
67.4		14.3	[27]
65.2	29.2		[28]
64.7	28.9	13.8	[29]
63.3–63.8	28.3	13.5	[43]
64.3	28.2	13.6	[30]

[a]Corrected by [29].

IV. DISCUSSION OF RESULTS

The preceding measurements on Si^{6+} and Si^{8+} [15] have reached an uncertainty close to 1% and at this level clearly discriminate among the available theoretical approximations. However, a measurement or calculation for a single ion species raises the question of reproducibility under a change of parameters. The comparison of measurement with calculational results can now be extended along the isoelectronic sequence to the ions of two more elements, with the level lifetimes roughly changing by a factor of 4 when changing the nuclear charge by merely two units. This has several advantages. The new data on $P^{7+,9+}$ and $S^{8+,10+}$ are even more precise by about a factor of 3, mostly because of better data statistics. Moreover, while experiment may suffer from unrecognized problems for a given element, theory is expected to provide smooth trends along the isoelectronic sequence. In

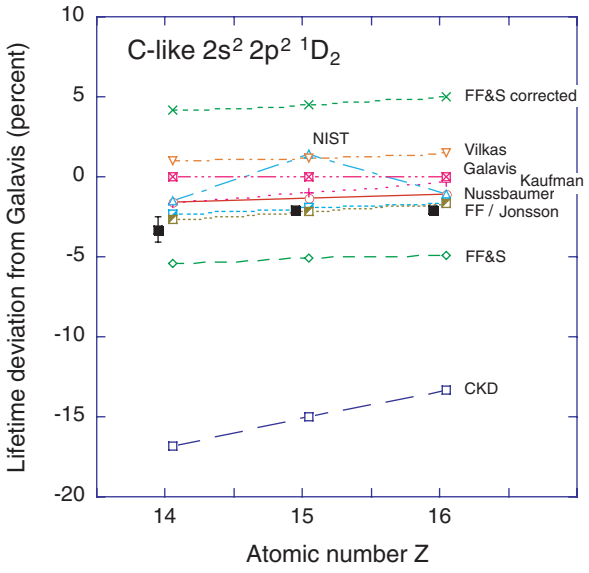

FIG. 3. (Color online) Deviation of the measured (Ref. [16] and this work) and predicted lifetimes of the $2s^2 2p^2\ {}^1D_2$ level in three C-like ions from the calculational results of Galavís *et al.* [29]. The symbols for the experimental data (solid squares with error bars, some of which do not exceed the symbol size) have been offset from the integer Z values for better clarity. References: CKD, Cheng, Kim, and Desclaux [24]; Nussbaumer: Nussbaumer and Rusca [32]; FF & S: Froese Fischer and Saha [34], also semiempirically corrected by Galavís *et al.* [29]; Kaufman: Kaufman and Sugar [26]; Vilkas: Vilkas *et al.* [35]; Galavis: Galavís *et al.* [29]; NIST: Ralchenko *et al.* [30]; FF: Froese Fischer and Tachiev [37]; and Jonsson: Jönsson *et al.* [38].

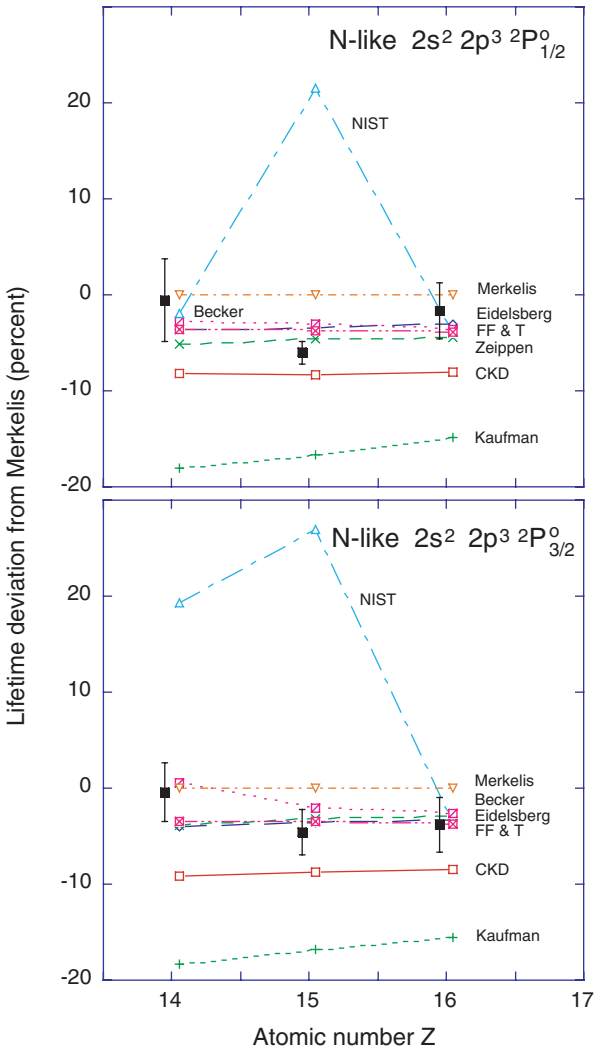

FIG. 4. (Color online) Deviation of the measured (solid squares with error bars, Ref. [16] and this work) and predicted lifetimes of the $2s^2 2p^3\ ^2P^o_{1/2,3/2}$ levels in three N-like ions from the calculational results of Merkelis *et al.* [42]. The symbols for the experimental data (solid squares with error bars) have been offset from the integer Z values for better clarity. References: CKD: Cheng, Kim, and Desclaux [24]; Eidelsberg: Eidelsberg *et al.* [4]; Zeippen [39]; Kaufman: Kaufman and Sugar [26]; Becker: Becker *et al.* [41]; NIST: Ralchenko *et al.* [30]; Merkelis: Merkelis *et al.* [42]; and FF & T: Froese Fischer and Tachiev [43].

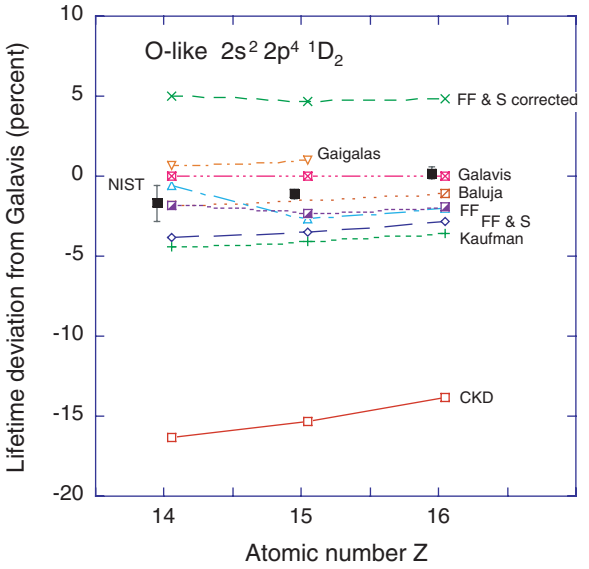

FIG. 5. (Color online) Deviation of the measured (Ref. [16] and this work) and predicted lifetimes of the $2s^2 2p^4\ ^1D_2$ level in three O-like ions from the calculational results of Galavís *et al.* [29]. The symbols for the experimental data (solid squares with error bars, some of which do not exceed the symbol size) have been offset from the integer Z values for better clarity. References: CKD: Cheng, Kim, and Desclaux [24]; FF & S: Froese Fischer and Saha [25], also semiempirically corrected by Galavís *et al.* [29]; Kaufman: Kaufman and Sugar [26]; Baluja: Baluja and Zeippen [27]; Gaigalas: Gaigalas *et al.* [28]; Galavis: Galavís *et al.* [29]; NIST: Ralchenko *et al.* [30]; and FF: Froese Fischer and Tachiev [43].

Figs. 3, 4, and 5 we compare the results of various calculations with our measured data. However, the calculational results depicted represent an incomplete selection; for example, Ref. [43] alone lists three more calculational data sets on C-like ions that have been obtained by different implementations of a basically similar approach, including one that replaces calculated energy level by measured data. Complete graphical presentations would be too dense to be of much use. We also leave out calculations that cover only a single ion of our sample. The results of some of the predictions are so close to each other that they cannot be separated graphically for all entries. However, for an isoelectronic survey the data swarm is of higher interest than the individual data which, anyway, are listed in the tables.

Most of the calculations of C- and O-like ions show a smooth isoelectronic trend of the difference to our chosen reference calculation by Galavís *et al.* [29], and some do not. This can be for various reasons. For example, Galavís *et al.* [29] have shown that the original results obtained by Froese Fischer and Saha [25,34] suffered from poor transition energies. After correcting those, the previously somewhat erratic isoelectronic trends became as flat (in comparison to the trend of their own results) as those of other calculations, albeit with a sizeable offset. The calculations by Galavís *et al.* [29] are rather close (less than 2% deviation) to our measured data. Moreover, the average distance would decrease further (by 0.45% of the total), if the long-overlooked QED correction to $M1$ transition amplitudes (for the electron anomalous magnetic moment (EAMM), see discussions in Refs. [10,11,13]) was applied (which seems to be missing in all calculations listed). Other sets of predictions have been obtained by Tachiev and Froese Fischer [36,37] and are summarized on their web site [43]. This summary is helpful and instructive; in a number of cases the results listed appear to have been obtained by calculations that exceed the work described in the references given. However, for the C-like ion Si^{8+} the three results obtained by the same authors span a band of 1.5% width that includes the result of the present measurement. Froese Fischer [44] discusses this scatter as a measure of accuracy of the techniques used, recognizing the limitations of theoretical approximations. Evidently experiment is called for to find out which set of calculations is best and how accurate it actually may be. Incidentally, we find the most recent calculations by

Froese Fischer [44] and by Jönsson *et al*. [38] to come closest to the experimental findings for C-like ions. For O-like ions, the situation is less clear, as the experimental data suggest an isoelectronic trend of a slightly different slope that crosses the trends of several calculations. Closest to experiment (on average) in this case are the results reported by Baluja and Zeippen [27] and Galavís *et al*. [29] and the most recent results of Froese Fischer and Tachiev [43].

For the N isoelectronic sequence we chose the many-body perturbation theory calculations by Merkelis *et al*. [42] for reference. Because of the fit problem of two not very different contributions to the decay curves, the measured lifetime data on N-like ions carry substantially larger error bars than the others, and the scatter of the results along the isoelectronic sequence is notable. While the data are quantitatively less significant than the lifetime data on the $^1D_2$ level in C- and O-like ions, the general situation is similar. On average, we find the early calculations by Eidelsberg *et al*. [4], Zeippen [39], and Becker *et al*. [41] and the recent ones by Froese Fischer and Tachiev [37] close to experiment. The values given in the NIST ASD database [30] evidently are isoelectronically inconsistent in this case, and the values obtained by Kaufman and Sugar [26] show an uncommon offset from the other calculations.

V. CONCLUSION

Theory spans a band of predictions for the transition rates of present interest that is roughly 5–10% wide (with some drastically different outliers and some inconsistent isoelectronic trends) and that encompasses the experimental lifetime data. However, experiment provides a much narrower band in all three isoelectronic sequences, with an uncertainty of 1% or less in the C- and O-like ions, challenging the accuracy that can be reached with present-day quantum-mechanical many-body calculations. In fact, the C- and O-like ions studied here are promising candidates to drive the experimental uncertainty of lifetime determinations to a small fraction of the QED correction of the $M1$ transition operator, in order to provide a "second opinion" on the discrepancy that has been found between the results of lifetime measurements on B- and Al-like ions at an electron beam ion trap [10–12] and current theory. There the same problem occurred as in analyzing the results of the present work: quantum-mechanical calculations have provided many numbers, but the question of accuracy of the various calculational approaches has not been addressed to the extent that the sizable QED contribution to the $M1$ transition amplitude could be tested. In the present measurements for a range of C-, N-, and O-like ions the experimental uncertainty is already smaller than this hitherto untested QED correction, opening a new path for a search for possibly new physics beyond the standard model.

ACKNOWLEDGMENTS

We are happy to acknowledge the dedicated technical support by the MP and TSR groups, which has been essential for this work. ET acknowledges financial support by the Deutsche Forschungsgemeinschaft (DFG). Support by the Max Planck Society is gratefully acknowledged.

[1] B. Edlén, Z. Astrophys. **22**, 30 (1942).
[2] B. Edlén, Phys. Scr., T **8**, 5 (1984).
[3] M. Kafatos and J. P. Lynch, Astrophys. J., Suppl. Ser. **42**, 611 (1980).
[4] M. Eidelsberg, F. Crifo-Magnant, and C. J. Zeippen, Astron. Astrophys. **43**, 455 (1981).
[5] E. Träbert, Phys. Scr. **61**, 257 (2000).
[6] E. Träbert, Phys. Scr., T **100**, 88 (2000).
[7] E. Träbert, Can. J. Phys. **80**, 1481 (2002).
[8] E. Träbert, Can. J. Phys. **86**, 73 (2008).
[9] E. Träbert, J. Phys. B: At. Mol. Opt. Phys. **43**, 074034 (2010).
[10] A. Lapierre *et al*., Phys. Rev. Lett. **95**, 183001 (2005).
[11] A. Lapierre *et al*., Phys. Rev. A **73**, 052507 (2006).
[12] G. Brenner, J. R. Crespo López-Urrutia, Z. Harman, P. H. Mokler, and J. Ullrich, Phys. Rev. A **75**, 032504 (2007).
[13] M. Nemouchi and M. Godefroid, J. Phys. B **42**, 175002 (2009).
[14] E. Träbert, J. Hoffmann, C. Krantz, A. Wolf, Y. Ishikawa, and J. A. Santana, J. Phys. B **42**, 025002 (2009).
[15] E. Träbert, A. Wolf, E. H. Pinnington, J. Linkemann, E. J. Knystautas, A. Curtis, N. Bhattacharya, and H. G. Berry, Can. J. Phys. **76**, 899 (1998).
[16] E. Träbert, A. G. Calamai, J. D. Gillaspy, G. Gwinner, X. Tordoir, and A. Wolf, Phys. Rev. A **62**, 022507 (2000).
[17] D. Habs *et al*., Nucl. Instrum. Methods Phys. Res., Sect. B **43**, 390 (1989).
[18] A. Müller and A. Wolf, in *Accelerator-Based Atomic Physics Techniques and Applications*, edited by S. M. Shafroth and J. C. Austin (Am. Inst. Phys., Washington, DC, 1997), p. 147.
[19] J. Doerfert, E. Träbert, A. Wolf, D. Schwalm, and O. Uwira, Phys. Rev. Lett. **78**, 4355 (1997).
[20] E. Träbert, A. Wolf, J. Linkemann, and X. Tordoir, J. Phys. B **32**, 537 (1999).
[21] G. Bisoffi *et al*., Nucl. Instrum. Methods Phys. Res., Sect. A **287**, 320 (1990).
[22] E. Träbert, Phys. Scr. **23**, 253 (1981).
[23] K. Omidvar, Phys. Rev. A **26**, 3053 (1982).
[24] K. T. Cheng, Y. K. Kim, and J. P. Desclaux, At. Data Nucl. Data Tables **24**, 111 (1979).
[25] C. Froese Fischer and H. P. Saha, Phys. Rev. A **28**, 3169 (1983).
[26] V. Kaufman and J. Sugar, J. Phys. Chem. Ref. Data **15**, 321 (1986).
[27] K. L. Baluja and C. J. Zeippen, J. Phys. B **21**, 1455 (1988).
[28] G. Gaigalas, J. Kaniaukas, R. Kisielius, G. Merkelis, and M. J. Vilkas, Phys. Scr. **49**, 135 (1994).
[29] M. E. Galavís, C. Mendoza, and C. J. Zeippen, Astron. Astrophys., Suppl. Ser. **123**, 159 (1997).
[30] Yu. Ralchenko, A. E. Kramida, J. Reader, and NIST ASD Team (2008), NIST Atomic Spectra Database (Version 3.1.5), available online at [http://physics.nist.gov/asd3].
[31] W. L. Wiese, M. W. Smith, and B. M. Glennon, *Atomic Transition Probabilities, Vol. I: Hydrogen through Neon* (US Government Printing Office, Washington, DC, 1966).

[32] H. Nussbaumer and C. Rusca, Astron. Astrophys. **72**, 129 (1979).
[33] K. L. Baluja, J. Phys. B **18**, L413 (1985).
[34] C. Froese Fischer and H. P. Saha, Phys. Scr. **32**, 181 (1985).
[35] M. J. Vilkas, I. Martinson, G. Merkelis, G. Gaigalas, and R. Kisielius, Phys. Scr. **54**, 281 (1996).
[36] G. Tachiev and C. Froese Fischer, Can. J. Phys. **79**, 955 (2001).
[37] C. Froese Fischer and G. Tachiev, At. Data Nucl. Data Tables **87**, 1 (2004).
[38] P. Jönsson, P. Rynkun, and G. Gaigalas, At. Data Nucl. Data Tables **97**, 648 (2011).
[39] C. J. Zeippen, Mon. Not. R. astron. Soc. **198**, 111 (1982).
[40] M. Godefroid and C. Froese Fischer, J. Phys. B **17**, 681 (1984).
[41] S. R. Becker, K. Butler, and C. J. Zeippen, Astron. Astrophys. **21**, 375 (1989).
[42] G. Merkelis, I. Martinson, R. Kisielius, and M. J. Vilkas, Phys. Scr. **59**, 122 (1999).
[43] C. Froese Fischer and G. Tachiev, MCHF/MCDHF Collection, Version 2, available online at [http://physics.nist.gov/mchf] (National Institute of Standards and Technology, 2011).
[44] C. Froese Fischer, Phys. Scr., T **134**, 014019 (2009).